Differences in SiC thermal oxidation process between crystalline surface orientations observed by in-situ spectroscopic ellipsometry

Daisuke Goto, Yasuto Hijikata, Shuhei Yagi, and Hiroyuki Yaguchi

Citation: Journal of Applied Physics **117**, 095306 (2015); doi: 10.1063/1.4914050
View online: http://dx.doi.org/10.1063/1.4914050
View Table of Contents: http://scitation.aip.org/content/aip/journal/jap/117/9?ver=pdfcov
Published by the AIP Publishing

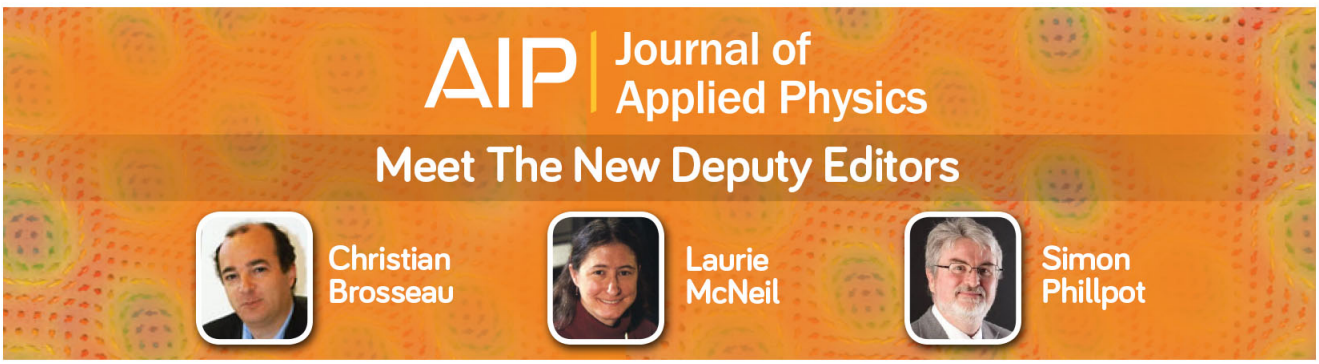

Differences in SiC thermal oxidation process between crystalline surface orientations observed by *in-situ* spectroscopic ellipsometry

Daisuke Goto, Yasuto Hijikata,[a] Shuhei Yagi, and Hiroyuki Yaguchi
Division of Mathematics Electronics and Information Sciences, Graduate School of Science and Engineering, Saitama University, 255 Shimo-Okubo, Sakura-ku, Saitama-city, Saitama 338-8570, Japan

(Received 18 December 2014; accepted 22 February 2015; published online 6 March 2015)

For a better understanding of the SiC oxidation mechanism, we investigated differences in the oxidation process for surfaces with different crystal orientations. Real-time observations of oxidation processes for (0001) Si-face, $(11\bar{2}0)$ *a*-face, and $(000\bar{1})$ C-face substrates at various oxidation temperatures were performed using *in-situ* spectroscopic ellipsometry. Massoud's empirical equation, which is composed of the classical Deal-Grove equation added by an exponential term, was applied to the observed growth rates and the oxidation rate parameters were extracted by curve fitting. The SiC oxidation mechanism is discussed in terms of the oxidation temperature dependence and surface orientation dependence of the oxidation rate parameters. © *2015 AIP Publishing LLC*. [http://dx.doi.org/10.1063/1.4914050]

I. INTRODUCTION

Recently, efficiency improvements for power devices are required all over the world for reducing energy consumption. Although Si has been used as a power device semiconductor, improving the performance of Si power devices can no longer be expected because the devices have reached their performance limit derived from the physical properties of Si. Silicon carbide (SiC), a wide bandgap semiconductor, has excellent physical properties for power device applications including a three times wider bandgap, three times higher thermal conductivity, and ten times larger breakdown field than Si. Therefore, SiC is expected to be a post Si power device material. In addition, SiO_2 can be grown on SiC surfaces by thermal oxidation, similar to Si. For these reasons, many studies on the practical uses of SiC metal-oxide-semiconductor field-effect-transistors (MOSFETs) have been carried out. However, the on-resistance for fabricated SiC-MOSFETs is higher than expected from the SiC properties and their channel mobility is severely low, which has been regarded as attributable to the interface states existing at/around the SiC–SiO_2 interface.[1] Furthermore, reliability characterizations for oxides on SiC show a one order lower charge-to-breakdown at a reliability of 50% less than that on Si.[2] Recent studies also revealed that C interstitials diffuse into 4H-SiC substrates and fill carbon vacancies, which are attributed to the origin of the $Z_{1/2}$ center.[3–5] Because it is believed that the SiC oxidation mechanism is closely related to the oxide quality, the interface structure and point defect elimination, observation of the SiC oxidation process is very important.

In previous studies, we performed real-time observations of SiC thermal oxidation using *in-situ* spectroscopic ellipsometery.[6–11] We found for the first time that the oxide growth rate rapidly decreases in the initial oxidation stage. We also found that Massoud's empirical equation[12] exhibits a better fit than the simple linear-parabolic Deal-Grove model.[13] This empirical equation was proposed for such an initial rapid deceleration in oxide growth on Si.[12] In addition, Kageshima *et al*. proposed a kinetic model that explains the initial growth rate deceleration, termed "interfacial Si emission model."[14] According to this model, Si interstitials are emitted into the oxide layer during oxidation and interfacial oxidation reaction is suppressed as the interstitials accumulate near the interface. For SiC oxidation, Hijikata *et al*. proposed a kinetic model that is based on the interfacial Si emission model, termed "Si and C emission model."[15] While in the case of SiC oxidation, they assumed that not only Si but also C interstitials are emitted into the oxide during oxidation and both kinds of interstitials prevent the interfacial oxidation reaction. We believe that examining the dependence of the oxidation process on the crystal surface orientation will provide valid information to the oxidation mechanism.

In this paper, we performed real-time observations of the thermal oxidation process on the (0001) Si face, $(11\bar{2}0)$ *a* face, and $(000\bar{1})$ C face at various temperatures and investigated oxidation process differences between these surface orientations.

II. GROWTH RATE EQUATION

One of the most popular oxidation models is the Deal-Grove (D-G) model,[13] which has been proposed in order to explain the Si oxidation process. According to this model, the relationship between the oxide thickness X and oxidation time t is expressed by the following equation:

$$X^2 + AX = B(t + \tau), \tag{1}$$

where B/A, B, and τ are the liner rate constant, the parabolic rate constant, and the constant related to initial oxide thickness, respectively. Equation (1) can be rewritten as the growth rate equation as follows:

[a]Tel./Fax: +81-48-858-3822. E-mail: yasuto@opt.ees.saitama-u.ac.jp

$$\frac{dX}{dt} = \frac{B}{A + 2X}. \tag{2}$$

As shown in Eq. (2), the linear rate constant B/A is the oxidation rate when $2X \ll A$, in which the interface oxidation reaction is the rate-limiting step. The oxide growth rate is expressed as $B/2X$ after the oxidation progresses ($2X \gg A$), and in this case the diffusion of oxygen in SiO_2 is the rate-limiting step. However, it is well known that the oxide growth rate cannot be characterized by the D-G model for thin oxide regions in Si[12] and SiC oxidation.[6,7,16]

Massoud *et al*. proposed an empirical relation for the oxide thickness dependence of the oxide growth rate for Si to represent the rates in a thin oxide regime.[12] This equation is obtained by adding an exponential term to the D-G relation, i.e.,

$$\frac{dX}{dt} = \frac{B}{A + 2X} + C\exp\left(-\frac{L}{X}\right), \tag{3}$$

where C and L are the exponential prefactor and the characteristic length, respectively. For SiC oxidation, it has been reported that Eq. (3) could reproduce the oxide growth rate better than Eq. (2).[6,7] Accordingly, we used Eq. (3) for curve fittings to obtain the oxidation rate parameters (B/A, B, C, and L).

III. EXPERIMENTS

4H-SiC (0001) Si-face (n type, $1.0 \times 10^{16}\,cm^{-3}$, 8° off), 6H-SiC ($11\bar{2}0$) a-face (n type), and 4H-SiC ($000\bar{1}$) C-face (n type, 0.5° off) substrates were used as samples. Note that the difference in growth rate due to that of polytype[17] or off-angle is within measurement errors. Oxidation was carried out using an infrared lamp heater at temperatures between 900 and 1230 °C, an oxygen flow of 1000 sccm, and an oxygen partial pressure of 1.0 atm. Before oxidation, the polarization parameters (Ψ, Δ) were measured under an Ar atmosphere at the oxidation temperature to determine the optical constants of SiC at the corresponding temperature. The Ar gas was then replaced with oxygen gas and real-time measurements of (Ψ, Δ) were started. We selected a wavelength range of 310–410 nm for oxide thickness analysis to avoid radiation or reflection light from the sample. The angle of incidence was 75.8°. When evaluating oxide thicknesses from (Ψ, Δ) spectra, we assumed a three-layer structure as an analysis model consisting of SiO_2/interface layer/SiC. Details of the analysis method are described elsewhere.[11,18]

IV. RESULTS

Figures 1(a)–1(c) show the oxide growth rate dependence of the oxide thickness for the Si face, a face, and C face, respectively, at various oxidation temperatures. The data points are measured values and the broken lines are fits using Massoud's empirical relation (Eq. (3)). At the same oxidation temperature, the oxide growth rate was fastest for the C face followed by a face and then the Si face. The fitted curves well reproduced the measured growth rates in the entire thickness range regardless of surface orientation and

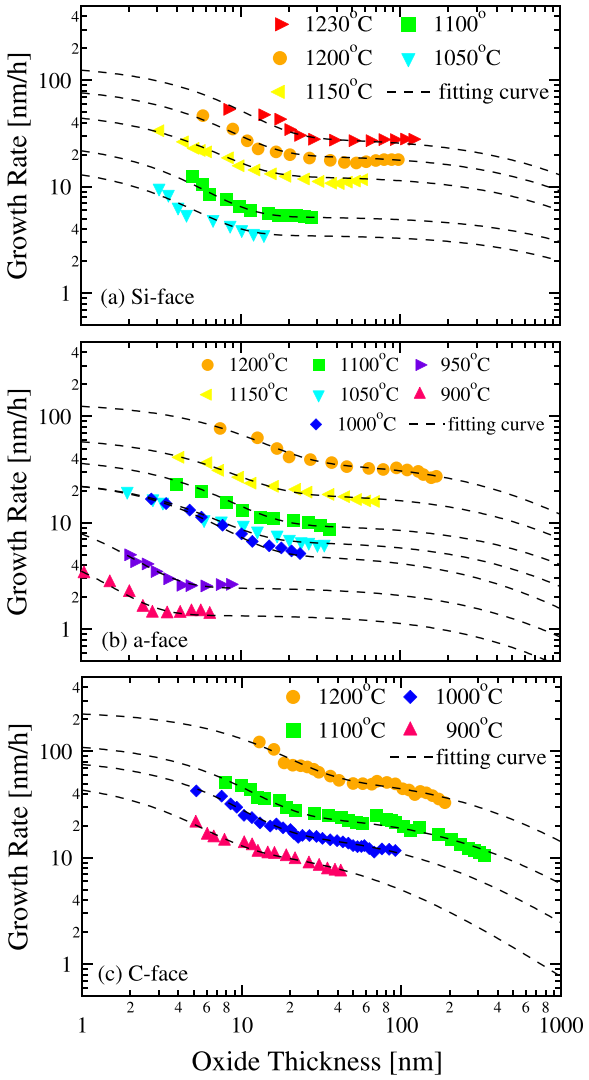

FIG. 1. Oxide thickness dependence of oxide growth rate at various temperatures on the (a) (0001) Si face, (b) ($11\bar{2}0$) a face, and (c) ($000\bar{1}$) C face.

temperature. Through the curve fitting, we determined the growth rate constants, i.e., the linear rate constant B/A, the parabolic rate constant B, the initial growth rate $B/A + C$, and the characteristic length L.

Figure 2 shows the temperature dependence of the linear rate constant B/A. The values of B/A mean the growth rates after the initial reduction for the C face and the a face are the largest and the second largest, respectively. From the fits to the observed values, B/A activation energies for the C face, a face, and Si face were found to be 0.72, 1.45, and 2.10 eV, respectively.

Figure 3 shows the temperature dependence of the initial growth rate $B/A + C$, which is the growth rate when the oxide thickness X is approximated to 0 in Eq. (3). The activation energies for the C face, a face, and Si face were 0.71, 1.43, and 2.15 eV, respectively. These values are nearly equal to those for B/A. It is considered that the $B/A + C$ parameter reflects the difference in surface oxidation reactions between surface orientations.

Figure 4 shows the temperature dependence of the parabolic rate constant B. From the figure, the value and activation energy of B do not depend on the surface orientation.

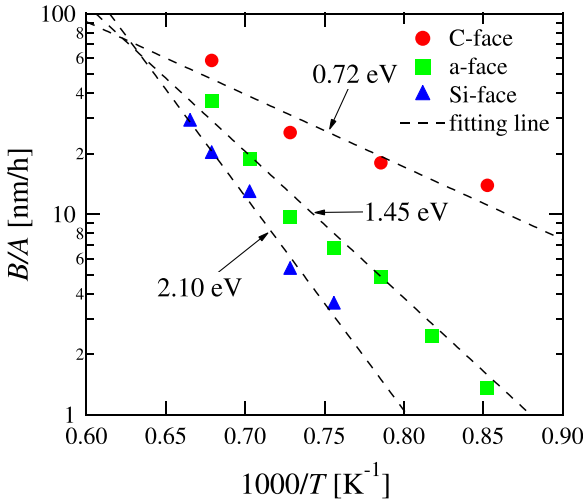

FIG. 2. Arrhenius plots for linear rate constant B/A.

Figure 5 shows the temperature dependence of the characteristic length L. From the figure, it is clear that L depends on temperature. Moreover, the characteristic lengths L are different between surface orientations, i.e., those for the C face are larger than those for the a face, which are both larger than those for the Si face.

V. DISCUSSION

In Figs. 2 and 3, it is clear that the activation energies of B/A and $B/A+C$ are nearly the same for each orientation. Moreover, it is interesting that the ratio of activation energies for the C face, a face, and Si face is close to 1:2:3. When Si atoms on a surface of a SiC substrate are oxidized, it is necessary to break one Si–C back-bond for the C face, two Si–C back-bonds for the a face, and three Si–C back-bonds for the Si face, as shown in Fig. 6. Because the ratio of activation energies correspond to the difference in the number of Si–C bonds broken between surface orientations, the energy for oxidation in the rate-limiting interface reaction, expressed by B/A or $B/A+C$, should relate to the energy for breaking a Si–C back-bond.

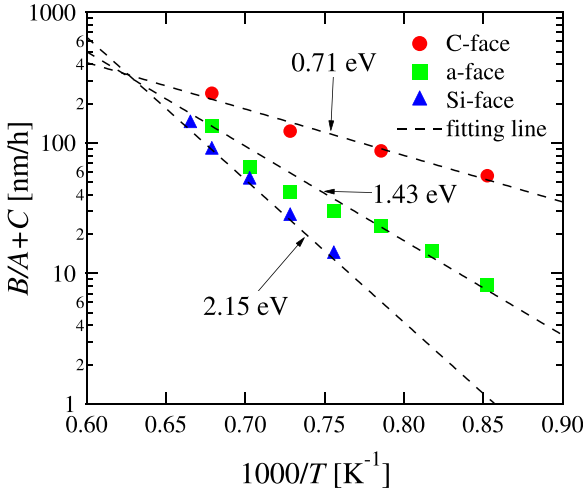

FIG. 3. Arrhenius plots for initial growth rate $B/A+C$.

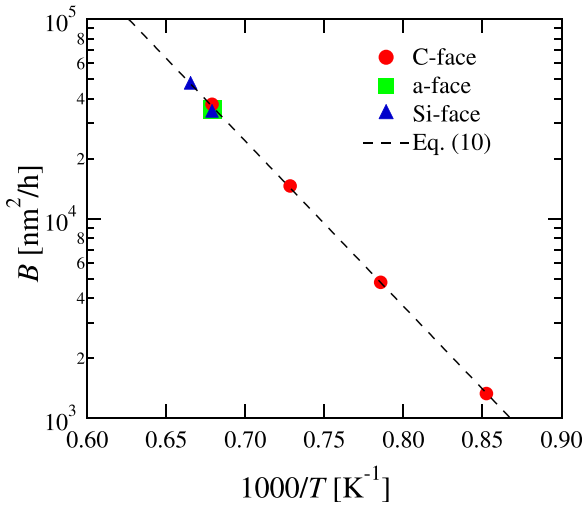

FIG. 4. Arrhenius plots for parabolic rate constant B.

The ratio of B/A and $B/A+C$, a deceleration ratio of steady oxide growth rate and initial oxide growth rate ($X \sim 0$), is approximately 1/5 irrespective of temperature and surface orientation. The deceleration ratio can be modified to the following equation:

$$\frac{B/A}{B/A+C} = \frac{1}{1+C/(B/A)} = \frac{1}{1+K}, \tag{4}$$

where $K = C/(B/A)$ and is a constant (i.e., 4) that is independent of temperature and surface orientation. Equation (3) can be approximated to the following equation in the interface reaction limiting-step ($X \ll A/2$) as:

$$\frac{dX}{dt} \approx \frac{B}{A} + C\exp\left(-\frac{X}{L}\right). \tag{5}$$

Thus, Eq. (5) can be rewritten as[19]

$$\frac{dX}{dt} = \frac{B}{A}\left\{1 + K\exp\left(-\frac{X}{L}\right)\right\}. \tag{6}$$

From Eq. (6), the oxide growth rate decelerates with an increasing oxide thickness from $B(1+K)/A$ to B/A in the

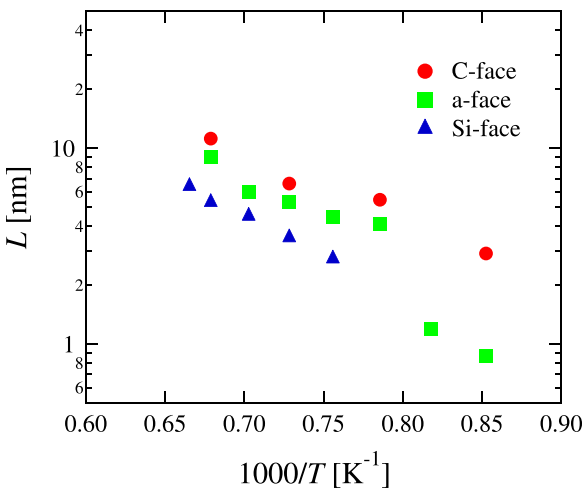

FIG. 5. Arrhenius plots for characteristic length L.

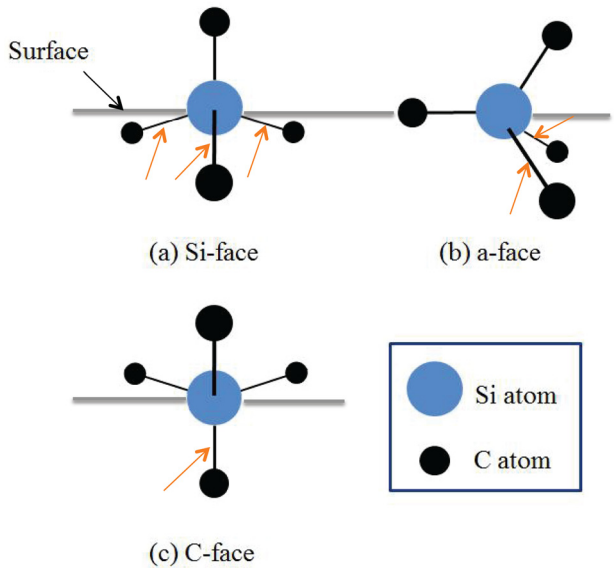

FIG. 6. Schematic diagrams of Si–C bonds on the SiC surface. The orange arrow denotes Si back-bond.

interfacial reaction limiting-step ($X \ll A/2$). According to the Deal-Grove model, oxide growth rate in the interfacial reaction limiting-step is expressed by the following equation:

$$\frac{dX}{dt} = \frac{B}{A} = \frac{k}{N_0} C_O^I, \tag{7}$$

where k is the interfacial reaction rate, N_0 is the molecular density of SiO_2, and C_O^I is the concentration of oxygen at the SiC–SiO_2 interface. In the Deal-Grove model, k and N_0 are constants and C_O^I is also constant (~oxygen solubility limit of SiO_2)[13] for the interfacial reaction limiting-step. Thus, the oxide growth rate should be constant in this region. However, from this study and previous studies,[6,7,16] it is obvious that the oxide growth rate decelerates in the interfacial reaction limiting-step. Since N_0 and C_O^I are theoretically independent of oxide thickness, temperature, and surface orientation in this oxide thickness region, k should decrease with oxide thickness. Recently, Hijikata *et al.* proposed an SiC oxidation model, termed "Si and C emission model"[15] and have discussed the SiC oxidation mechanism.[20–24] According to this model, the accumulation of Si and C interstitials emitted from the SiC–SiO_2 interface during oxidation causes interfacial oxidation reaction prevention, and thereby the oxide growth rate decreases rapidly in the initial oxidation stage. To describe this initial deceleration process, they gave an interfacial reaction rate that decreases as oxidation progresses, i.e.,

$$k = k_0 \left(1 - \frac{C_{Si}^I}{C_{Si}^0}\right)\left(1 - \frac{C_C^I}{C_C^0}\right), \tag{8}$$

where k_0 and C^0 are the initial interfacial reaction rate and solubility limit in SiO_2, respectively. Substituting Eq. (8) in Eq. (7) and in comparison to Eq. (6), a decreasing k is more reasonable than a constant k. As mentioned above, the growth rate reduces from $B(1+K)/A$ to B/A with an increasing oxide thickness. Therefore, k/k_0 in Eq. (8) should vary from 1 to $1/(1+K)$. The validity of this will be investigated elsewhere.

The characteristic length L is the oxide thickness when the growth rate for the initial deceleration region levels off. According to the Si and C emission model,[15] L is considered as the oxide thickness at which the accumulation and consumption of interstitials balance. It suggests that this parameter is determined by the oxidation coefficient and the diffusion coefficient of SiO_2 interstitials and the emission ratios of Si and C interstitials. These values should be larger at higher temperatures. Thus, an increase in the diffusion coefficient leads to an increase in L. In contrast, an increase in the SiO_2 oxidation coefficient or the emission ratio of interstitial leads to a reduction in L. Therefore, the results in Fig. 5 suggest that an increase in the diffusion coefficient due to an increase in temperature is more significant than the other two correlations. Additionally, it has been reported that the activation energy for the diffusion coefficient is higher than the other two activation energies.[25] It is also believed that the interstitials emission ratio depends on surface orientation in SiC oxidation as well as Si oxidation.[21,25] As mentioned before, L decreases if the atomic emission ratio is large, and thus the results in Fig. 5 are consistent with the prediction that the emission ratio for the Si face is significantly larger than that for the C face.[21]

Fig. 4 suggests that the oxidation process in thick regions ($X \gg A/2$) is independent of the surface orientation. Since the thermal oxide is SiO_2 regardless of surface orientation, and the growth rate is determined by the nature of SiO_2 in this region, it is reasonable that the value of B (i.e., diffusivity of oxygen or carbonaceous products in SiO_2) is identical between surface orientations. Here, we assume that the oxidation reaction of SiC is represented by the following chemical equation:

$$SiC + \frac{3}{2}O_2 \rightarrow SiO_2 + CO. \tag{9}$$

Since SiC oxidation consumes 1.5 times the amount of oxygen than for Si, the value of B is 1/1.5 of that of Si. In Si oxidation, the value of B can be expressed with oxygen self-diffusivity in SiO_2, $D^{SD}{}_O$.[26] Accordingly, the B value for SiC is assumed to be

$$B = \frac{2D^{SD}{}_O}{1.5} = \frac{2 \times 3.20 \times 10^{-8}}{1.5} \exp\left(-\frac{1.64\text{eV}}{k_B T}\right), \tag{10}$$

where k_B and T indicate the Boltzmann constant and absolute temperature, respectively. The broken line in Fig. 4 is the calculated B value obtained from Eq. (10). The figure shows that the measured values are in good agreement with the calculated line. Therefore, the in-diffusion of oxygen in SiO_2 is a rate-limiting step in this thick region and C atoms in SiC outgas as CO during oxidation, irrespective of surface orientation, which is consistent with recent work.[27]

Figure 7 shows the time dependence data of the oxide thickness in these experiments. This consolidated our

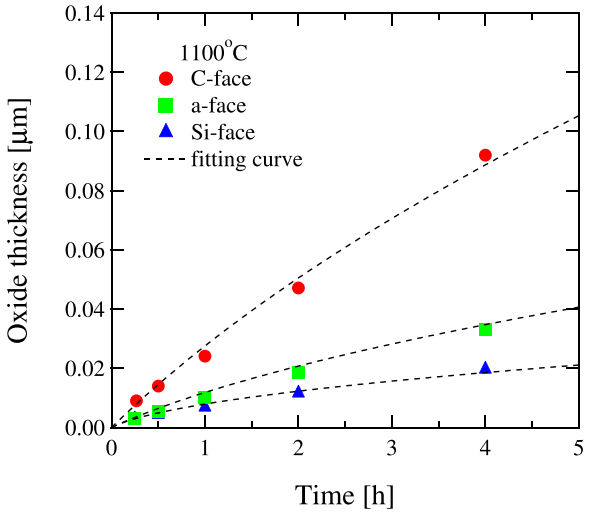

FIG. 7. Oxidation time dependence of oxide thickness at various temperatures.

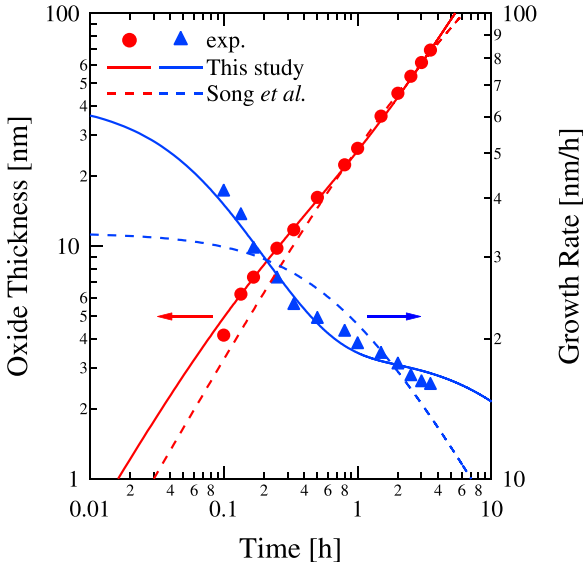

FIG. 9. Time dependence of oxide thickness and oxide growth rate at 1150 °C on *a* face with curves obtained using Eq. (3) (solid line) and by the Song *et al*. method (broken line).

measured data to be equivalent to the data from Song *et al*.[28] We fit curves to this data with $\tau = 0$ in Eq. (1) following the report from Song *et al*. The broken lines in Fig. 7 show the fits using Eq. (1), which reproduce the measured values reasonably well.

Figure 8 shows Arrhenius plots of the (a) linear rate constant B/A and (b) parabolic rate constant B obtained from the fits, as shown in Fig. 7. The activation energies for B/A were comparable between the surface orientations, but the values were different from each other. The values for B are dependent on surface orientation while the activation energy for the C face was different from the other surface orientations. These results do not agree with the results shown in Figs. 2 and 4, but the activation energies for B/A and B were mostly equal to those reported.[28] Therefore, there is no significant difference in the measured data between ours and Song *et al*. Namely, we found that the obtained growth rate parameters are vastly different in accordance to the fitting functions and fitting targets (oxide thickness data or growth rate data).

Song *et al*. proposed a modified Deal-Grove model for the thermal oxidation of SiC, i.e., the parameter B multiplied by a factor due to the outgassing of CO during SiC oxidation is taken into account.[28] Other parts are completely equivalent to the D-G model. Hence, the activation energy for the linear rate constant B/A should correspond to the surface oxidation rate for the surface orientation. However, as shown in Fig. 8, the energies for B/A are comparable between these surface orientations. In addition, it is also notable that the activation energies of parabolic rate constants B are different between surface orientations. Because oxide grown on SiC surfaces is SiO_2 irrespective of the surface orientation, nearly the same oxidation process should proceed for the diffusion rate-limiting step ($X \gg A/2$). It is possible that the production ratio of C, CO, and CO_2 varies with surface orientation and that the coefficient for O_2 in Eq. (9) is different. However, the coefficient is within a range from 1 to 2. Therefore, the large difference in B values depending on surface orientation as shown in Fig. 8 should not arise and the activation energies of B should be the same. In addition, looking at the line calculated by Eq. (10), B values in Fig. 8 are much smaller than those obtained in this study. Although the growth rate in thick thickness region for Si and *a* face could not sufficiently be obtained in the experiments, it can be safely said that such a small B values cannot be correct because the thickness of $A/2$ becomes less than 10 nm in this case. From this reason, the parameters obtained in this study are more reasonable than those from Song *et al*. Figure 9 shows the

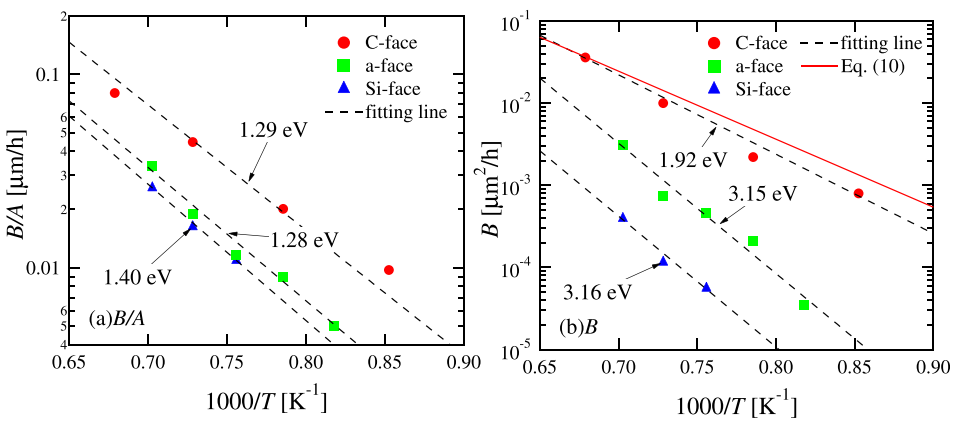

FIG. 8. Arrhenius plots for (a) linear rate constant B/A and (b) parabolic rate constant B obtained by the Song *et al*. method.

time dependence of the oxide thickness (circles) and oxide growth rate (triangles) at 1150 °C on the *a* face with a curve obtained using Eq. (3) (solid line) and by the Song *et al.* method (broken line). Although there was not a huge deviation between the observed oxide thicknesses and the curve fits for the two methods, the growth rate curve deviation from our method was much smaller. In the Song *et al.* method, since the initial deceleration is ignored, the oxide thickness region after several tens of nanometers seems to be regarded as the diffusion rate-limiting step. In conclusion, it is clear that more reasonable analysis can be carried out for use of the fitting function with initial deceleration and dense growth rate data.

VI. SUMMARY

To investigate the differences of SiC oxidation processes due to surface orientation, we performed real-time observations of the oxidation process on the Si face, *a* face, and C face and discussed the oxidation mechanism from the obtained growth rates and their dependence on temperature. The oxide growth rates during the interface reaction rate-limiting step depend on surface orientation, and the difference of their activation energies was consistent with the differences in the number of Si back-bonds in SiC. The growth rate during the diffusion rate-limiting step was found to be common irrespective of surface orientation, which can be explained by the diffusion of oxygen in SiO_2 being the rate-limiting step, and C atoms in SiC substrates are outgassed as CO. In addition, using the growth rate equation while taking the initial deceleration into account with the dense growth rate data, more accurate growth rate curves and appropriate oxidation rate parameters were obtained.

ACKNOWLEDGMENTS

The authors thank Dr. Nishino of Kyoto Institute of Technology for providing us a (11–20) *a*-face substrate. This work was supported in part by Grants-in-Aid for Scientific Research from Japan Society for the Promotion of Science (#24560365).

[1]G. Y. Chung, C. C. Tin, J. R. Williams, K. McDonald, R. K. Chanana, A. Weller, S. T. Pantelides, L. C. Feldman, O. W. Holland, M. K. Das, and J. W. Palmour, IEEE Electron Device Lett. **22**, 176 (2001).
[2]J. Senzaki, K. Kojima, and K. Fukuda, Appl. Phys. Lett. **85**, 6182 (2004).
[3]T. Hiyoshi and T. Kimoto, Appl. Phys. Express **2**, 091101 (2009).
[4]L. S. Løvlie and B. G. Svensson, Phys. Rev. B **86**, 075205 (2012).
[5]T. Miyazawa and H. Tsuchida, J. Appl. Phys. **113**, 083714 (2013).
[6]T. Yamamoto, Y. Hijikata, H. Yaguchi, and S. Yoshida, Jpn. J. Appl. Phys., Part 1 **46**, L770 (2007).
[7]T. Yamamoto, Y. Hijikata, H. Yaguchi, and S. Yoshida, Jpn. J. Appl. Phys., Part 1 **47**, 7803 (2008).
[8]T. Yamamoto, Y. Hijikata, H. Yaguchi, and S. Yoshida, Mater. Sci. Forum **600–603**, 667 (2009).
[9]Y. Hijikata, H. Yaguchi, and S. Yoshida, in *Properties and Applications of Silicon Carbide*, edited by R. Gerhardt (InTech, 2011), Chap. 4, p. 77.
[10]K. Kouda, Y. Hijikata, S. Yagi, and H. Yaguchi, Mater. Sci. Forum **645–648**, 813 (2010).
[11]K. Kouda, Y. Hijikata, S. Yagi, and H. Yaguchi, J. Appl. Phys. **112**, 024502 (2012).
[12]H. Z. Massoud, J. D. Plummer, and E. A. Irene, J. Electrochem. Soc. **132**, 2685 (1985).
[13]B. E. Deal and A. S. Grove, J. Appl. Phys. **36**, 3770 (1965).
[14]H. Kageshima, K. Shiraishi, and M. Uematu, Jpn. J. Appl. Phys., Part 2 **38**, L971 (1999).
[15]Y. Hijikata, H. Yaguchi, and S. Yoshida, Appl. Phys. Express **2**, 021203 (2009).
[16]E. A. Ray, J. Rozen, S. Dhar, L. C. Feldman, and J. R. Williams, J. Appl. Phys. **103**, 023522 (2008).
[17]C. Raynaud, J. Non-Cryst. Solids **280**, 1 (2001).
[18]H. Seki, Y. Hijikata, H. Yaguchi, and S. Yoshida, Mater. Sci. Forum **615**, 505 (2009).
[19]H. Z. Massoud and J. D. Plummer, J. Appl. Phys. **62**, 3416 (1987).
[20]Y. Hijikata, H. Yaguchi, and S. Yoshida, Mater. Sci. Forum **600–603**, 663 (2009).
[21]Y. Hijikata, H. Yaguchi, and S. Yoshida, Mater. Sci. Forum **645–648**, 809 (2010).
[22]Y. Hijikata, H. Yaguchi, and S. Yoshida, Mater. Sci. Forum **679–680**, 429 (2011).
[23]Y. Hijikata, H. Yaguchi, and S. Yoshida, Mater. Sci. Forum **740–742**, 833 (2013).
[24]Y. Hijikata, S. Yagi, H. Yaguchi, and S. Yoshida, in *Physics and Technologies of Silicon Carbide Devices*, edited by Y. Hijikata (InTech, 2013), Chap. 7, p. 181.
[25]M. Uematsu, H. Kageshima, and K. Shiraishi, J. Appl. Phys. **89**, 1948 (2001).
[26]H. Kageshima, M. Uematu, and K. Shiraishi, Microelectron. Eng. **59**, 301 (2001).
[27]R. H. Kikuchi and K. Kita, Appl. Phys. Lett. **105**, 032106 (2014).
[28]Y. Song, S. Dhar, L. C. Feldman, G. Chung, and J. R. Williams, J. Appl. Phys. **95**, 4953 (2004).